# MULTI-OBJECTIVE OPTIMIZATION OF A SOLAR HEAT PUMP SYSTEM USING PVT AND ICE-BASED LATENT STORAGE

**Justin Tamasauskas[1], Michel Poirier[1] and Radu Zmeureanu[2]**

[1] CanmetENERGY/Natural Resources Canada, Varennes, Canada

[2] Dept. of Building, Civil, and Environmental Engineering, Concordia University, Montreal, Canada

**Abstract**

This paper examines the optimization of a novel solar heat pump concept according to the competing objective functions of lifecycle energy and cost. First, the system concept is presented, combining photovoltaic/thermal collectors with ice storage and a heat pump to provide space and hot water heating. Next, the optimization methodology is discussed, including selected decision variables and optimization algorithm. Results for a high performance home in Montreal, QC, Canada, show a clear tradeoff between reduced lifecycle energy and increased costs, with the addition of PVT panels shown to be the main driver between solutions in the Pareto set. An additional case study explores the optimal balance between photovoltaic and photovoltaic/thermal collectors, and demonstrates the advantages of a properly sized system in comparison to a conventional heat pump using only photovoltaics.

*Keywords: Heat Pump, PVT, Thermal Storage, Multi-Objective Optimization*

## 1. Introduction

Heat pumps are widely recognized as key components of high performance buildings (IEA HPC, 2012), efficiently addressing thermal loads while facilitating the integration of renewable energy into the building. However, conventional air-source heat pumps experience a significant degradation of performance at colder ambient temperatures, presenting a major challenge in cold climates such as Canada. As such, alternative thermal sources must be considered in order to maximize heat pump performance during the coldest winter months.

Combining solar thermal and heat pump technologies has demonstrated strong potential to reduce building energy use and improve renewable energy fractions. However, a major challenge associated with these types of systems is the strong temporal discrepancy between solar availability and thermal demands. Several authors have proposed the use of ice-based thermal storage to address this issue (Trinkl et al., 2009; Tamasauskas et al., 2012; Dott & Afjei, 2014; Carbonell et al., 2016), with potential benefits including smaller storage volumes and improved solar collector efficiencies. These advantages are especially interesting when coupled with photovoltaic/thermal panels (PVT), where low temperature fluid from the ice tank can simultaneously cool photovoltaic modules to improve electrical efficiencies while also recovering low-grade thermal energy for use by the heat pump. In order for these types of systems to achieve a significant market share, it is vital that designers carefully balance energy and economic performance throughout the planned lifecycle.

Multi-objective optimization techniques are an important tool for exploring the design space and identifying trade-offs in competing objectives. More commonly applied to building form and envelope selection, the use of these techniques for sizing solar thermal and PVT systems is still relatively limited in the literature. For solar combi-systems, Bornatico et al. (2012) used a weighted sum approach to optimize three competing objective functions, while Ng Cheng Hin and Zmeureanu (2014) compared optimization results using three different objective functions. Rey and Zmeureanu (2016) later built upon this work by applying a multi-objective particle swarm approach to simultaneously optimize lifecycle cost and energy. However, to date, there has been limited systems level optimization of PVT-assisted heat pumps, especially for cold climates such as Canada.

This paper applies a multi-objective optimization algorithm to the sizing of a solar heat pump system using ice storage and PVT panels. First, the proposed concept is introduced, along with key modes of operation. Next, the optimization problem is formulated, followed by a presentation of the simulation methodology employed. Finally, results are provided for a high performance home in Montreal, Canada, with several solutions from the Pareto front examined to better understand the performance of the selected algorithm.


doi:10.18086/eurosun2018.02.05 Available at http://proceedings.ises.org

## 2. System Concept and Operations

The proposed system is shown in Figure 1, based on the work of Tamasauskas et al. (2016). The system operates year round to serve heating and DHW loads in the building.

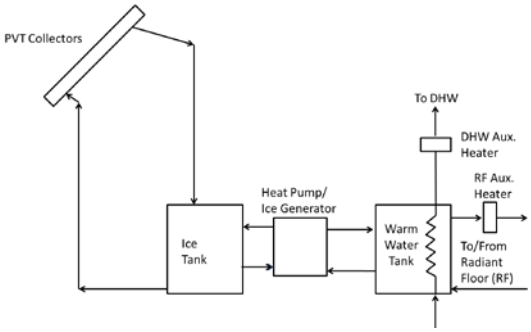


**Figure 1: Proposed system concept**

### 2.1 System Description

The system concept integrates liquid-based PVT with ice storage and heat pump technologies. Combining these technologies offers three key advantages:

I. *Improved Thermal and Electrical PVT Efficiencies*. Using ice storage allows a colder temperature fluid to be circulated to the PVT collectors. This minimizes thermal losses from the collector array, and provides effective cooling of the PV cells in order to maximize electrical efficiencies.

II. *Increased Energy Storage Densities*. The latent heat available during the ice/water phase change (333 kJ/kg) increases energy storage densities vs. sensible-only storage, minimizing tank volumes.

III. *Stable Heat Pump Operations*. Ice storage places a lower limit on the source temperature for the heat pump. This allows for more efficient heat pump operations, especially in comparison to conventional air-source heat pumps in cold climates such as Canada, where outdoor temperatures can often fall to -30°C during the winter months.

A PVT array (liquid based, using either glazed or unglazed collectors) on the south facing roof of the building acts as the primary source of thermal energy. Low-grade thermal energy obtained from the PVT collectors is then stored in ice tank. Ice storage is based on the use of ice slurry (a mixture of small diameter ice particles and water), with the ice tank operated in a non-agitated configuration to allow ice and water to separate via buoyancy into two distinct layers (Tamasauskas et al., 2012). Energy stored in the ice tank is upgraded by a water-water heat pump/ice generator for use in radiant flooring and domestic hot water (DHW) loops. Auxiliary electric heaters in the radiant floor and DHW loops supplement system operations as needed. All systems are electrically based to facilitate the use of electricity generated by the PVT panels, with no additional connections for natural gas or other fuel sources.

### 2.2 System Control

Control of the system is best understood in terms of three main loops:

*Solar Loop Control*: The solar loop is responsible for circulating fluid between the PVT collectors and ice tank. Loop operations are based on the following variables:

i. Useful Solar Gains. A *predicted* fluid temperature rise ($\Delta T_{Col,I}$) exceeding 3°C is required to start the solar loop pump. This ensures that the loop only operates when suitable solar gains into the system are available. Loop operations continue as long as the *actual* temperature rise (under flow conditions) remains above 1°C.

ii. Ice Tank Fluid Temperature. A maximum average fluid temperature of 26°C is defined for the ice tank ($T_{Fluid,IT}$), based on available heat pump information (ClimateMaster, 2010).

*Heat Pump Loop Control*: Heat pump control is based on the following variables:

i. Ice Mass in Ice Tank. The heat pump is allowed to operate if the ice mass in the ice tank is below a defined maximum ($M_{Ice,Max}$). This maximum has been set at 60% of the tank fluid mass, based on the maximum fraction obtained during experiments on a test bench system (Tamasauskas et al., 2016).

ii. Fluid Temperature in Warm Tank. The heat pump maintains a 45°C temperature at the top of the warm water tank ($T_{Fluid,WT}$).

A summary of the control parameters required to operate both the solar and heat pump loops is provided below in Table 1.

**Table 1: Summary of Solar and Heat Pump Control Loops**

| | | Control Parameters |
|---|---|---|
| Solar Loop | Heat Season | $\Delta T_{Col,I}$>3°C, $T_{Fluid,IT}$<26°C |
| Heat Pump | Heat Season | $M_{Ice}$<$M_{Ice,Max}$, $T_{Fluid,WT}$<45°C |

*Radiant Floor Loop Control*: The radiant flooring loop meets the space heating loads of each level of the building. Space air temperatures are maintained at 21°C for the two above ground floors, and 18°C for the basement. Fluid supply temperatures are varied with an outdoor air reset, ranging from 40°C at design conditions to 25°C at an ambient temperature of 18°C.

## 3. Optimization Formulation

A multi-objective optimization has been performed to determine tradeoffs in system sizing over a lifecycle of 40 years (Leckner, 2008). This section formulates the multi-objective optimization problem, including a presentation of the selected decision variables, objective functions and algorithm.

### *3.1 Decision Variables*

Decision variables used in the optimization focus on the thermal supply and storage capabilities of the system, and are summarized in Table 2. Maximum values for the storage tank volumes and number of solar collectors are based on available space within the building, with the maximum number of solar collectors varying by type due to the slightly smaller size of the unglazed collectors vs. the glazed ones. The range of specific flow rates used for the PVT collectors is selected based on information provided by the panel manufacturer (Solimpeks, 2014). Product lifecycles are used to identify when and how many times a piece of equipment must be replaced during the 40-year system lifecycle.

**Table 2: Summary of optimization decision variables**

| Variables | Type | Min | Max | Product Lifecycle (Years) |
|---|---|---|---|---|
| # PVT Collectors, Glazed ($N_{PVT}$, -) | Discrete | 1 | 29 | 25 |
| # PVT Collectors, Unglazed ($N_{PVT}$, -) | Discrete | 1 | 31 | 25 |
| Volume Ice Tank ($V_{IT}$, $m^3$) | Continuous | 0.3 | 5 | 15 |
| Volume Warm Tank ($V_{WT}$, $m^3$) | Continuous | 0.3 | 5 | 15 |
| Collector Spec Flow ($\dot{m}_{col}$, kg/s·$m^2$) | Continuous | 0.007 | 0.035 | 10 (Circ. Pumps) |

### *3.2 Objective Functions*

The optimization problem is based on the minimization of both lifecycle energy (LCE) and lifecycle cost (LCC). Details regarding each objective function is provided below.

*Lifecycle Cost (LCC)*. The lifecycle cost analysis focused on three main elements:

I. Initial purchase and installation of equipment associated with each decision variable

II. Purchase and installation of replacement equipment at end of equipment lifecycle, and

III. Utility costs associated with system operations over the defined lifecycle.

Mathematically, total lifecycle costs can be written as:

$$LCC = PW_{In} + PW_{Rep} + PW_{Ops} \quad \text{(eq. 1)}$$

Where $PW_{In}$, $PW_{Rep}$, and $PW_{Ops}$ are the initial, replacement, and operating costs, respectively, discounted to the start of the analysis period in $CAD. Future cash flows were discounted to present worth using an inflation rate of 1.45% and a nominal discount rate to 2.88%, based on the current Canadian financial market.

The costs associated with each decision variable are summarized in Table 3.

**Table 3: Summary of equipment costs associated with decision variables**

| Component | Cost (Equipment + Install, $ CAD) | Source |
|---|---|---|
| PVT Collector (Glazed) | $1028*N_{PVT}$ | Equipment: Haus Und Solar, 2016<br>Installation: RS Means, 2013 |
| PVT Collector (Unglazed) | $0.95*1028*N_{PVT}$ | Equipment: Haus Und Solar, 2016<br>Renewable Energy Hub, 2018<br>Installation: RS Means, 2013 |
| PV Panel | $584*N_{PV}$ | Equip./Install: EnergyHub.org, 2018 |
| Warm Tank | $2870*V_{WT}+995$ | Equip./Install: Ng Cheng Hin, 2013 |
| Ice Tank | $2870*V_{IT}+995$ | Equip./Install: Ng Cheng Hin, 2013 |
| Solar Circulation Pump | $8.27*P_{Rated}+168.68$, if $P_{Rated}<93W$<br>$0.56*P_{Rated}+901.61$, if $P_{Rated}\geq 93W$ | Equip./Install: RS Means, 2013 |

Where $N_{PV}$ is the number of PV panels, and $P_{Rated}$ is the rated pump power (W)

Utility costs are summarized in Table 4, based on current rates and structures for the Montreal region (Hydro Quebec, 2017). Fixed daily costs are neglected, as these remain the same for all systems. Only electrical utilities are presented, as all systems are electrically based. Escalation rates are derived from the five-year average for Montreal.

**Table 4: Utility rates for Montreal region**

| Variable | Tier | Value |
|---|---|---|
| Electricity Rate | First 30 kWh/day | 5.71 ₡/kWh |
| | Above 30 kWh/day | 8.68 ₡/kWh |
| Escalation Rate | - | 1.80% |

Lifecycle Energy. Lifecycle energy examines both:

I. The embodied energy of each component associated with a decision variable, and

II. The energy use of the system over its complete lifecycle.

Mathematically, this can be written as:

$$LCE = E_{Emb,I} + E_{Emb,R} + E_{Ops} \qquad \text{(eq. 2)}$$

Where $E_{Emb,I}$ is the embodied energy of the initial components (kWh), $E_{Emb,R}$ is the embodied energy of any replacement components (kWh), and $E_{Ops}$ is the energy use of the system over the 40 year lifecycle (kWh).

Table 5 summarizes the embodied energy of each system component involved in the optimization. For the PVT collectors, little information was available regarding embodied energy. As such, an expression was derived using information from Ng Cheng Him (2013) for a glazed solar thermal collector, and Leckner (2008) for a monocrystalline PV panel, as used in the selected PVT collectors. For the unglazed case, the embodied energy associated with the glass panel is subtracted from the glazed expression. Pump embodied energy is based on the use of a cast iron as the main component material.

**Table 5: Embodied energy associated with decision variables**

| Component | Lifecycle Energy (kWh) | Source |
|---|---|---|
| PVT Coll. | Gl: $2012*A_{PVT}*N_{PVT}+63.5*N_{PVT}+675$<br>UG: $1951*A_{PVT}*N_{PVT}+63.5*N_{PVT}-+675$ | Solar Thermal: Ng Cheng Him (2013)<br>Glazing: Chow & Ji, 2012 |
| PV | $1496*A_{PV}*N_{PV}$ | Leckner (2008) |
| Warm Tank | $1960*V_{WT}^{0.6}$ | Ng Cheng Hin (2013) |
| Ice Tank | $1960*V_{IT}^{0.6}$ | Ng Cheng Hin (2013) |
| Solar Pump | $M_{pump}*(32.8*0.28)$ | Derived via Spence & Kultermann (2017) |

Where $A_{PV}$ is the area of a PV panel, $N_{PV}$ is the number of PV panels, and $M_{Pump}$ is the mass of the pump (kg)

Operational energy is defined as the total energy use of the home, and can be written as:

$$E_{Ops} = N_{Lifecycle}\left(E_{HP} + E_{Aux} + E_{FansPumps} + E_{LightRecp} - E_{PV}\right) \quad \text{(eq. 3)}$$

Where $N_{Lifecycle}$ is the total lifecycle of the system (years), $E_{HP}$ is the annual energy use of the heat pump (kWh), $E_{Aux}$ is the annual energy use for auxiliary heating in the heating and DHW loops (kWh), $E_{FansPumps}$ is the annual energy use for pumps and fans (kWh), $E_{LightRecp}$ is the annual energy use for lights and receptacles (kWh), and $E_{PV}$ is the annual electricity generated from the PV array, PVT array, or both (kWh).

### 3.3 Optimization Algorithm

The non-dominated sorting genetic algorithm (NSGA-II) was selected to develop the Pareto front (Deb et al., 2002) due to its widespread use in building simulation and HVAC system sizing problems, and its availability in several common optimization packages such as MOBO (Palolen et al., 2013) and Matlab (Mathworks, 2018). A summary of key optimization parameters is provided in Table 6, based mainly on those recommended by Palolen et al. (2013).

**Table 6: Optimization algorithm parameters**

| Parameter | Value |
|---|---|
| Population Size | 16 |
| No. of Generations | 40 |
| Mutation Probability | 0.034 |
| Crossover Probability | 0.9 |

## 4. Simulation Methodology

TRNSYS v.17 (Klein et al., 2010) and the multi-objective optimization program MOBO (Palonen et al., 2013) were linked to perform the study. The two programs shared information as shown in Figure 2. At each generation, MOBO created a series of TRNSYS input files (one for each member of the population) using the set of decision variable values associated with each candidate in the population. TRNSYS then performed annual simulations for each population member, and reported the corresponding lifecycle cost and energy use back to MOBO. Finally, MOBO used this data to support the NSGA-II algorithm in its selection process in order to develop the next generation of candidate points.

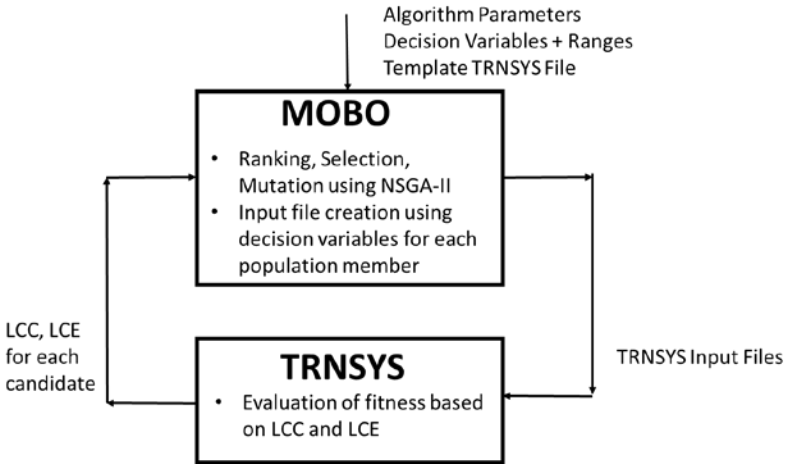


**Figure 2: Simulation architecture using MOBO and TRNSYS**

The remainder of this section examines the components used in TRNSYS.

## 4.1 TRNSYS System Simulations

TRNSYS was selected for all system simulations because of its ability to simulate the complex and unique HVAC system proposed in this work. All models were simulated at a time step of 3.75 minutes, with this small time step required to appropriately model system control decisions and promote solution convergence in TRNSYS. The choice of 3.75 minutes has also been specifically chosen because this time step is of the form 1/2*n* hours (where *n* is a user-selected integer), which ensures that there are no issues with TRNSYS components writing data to external files (Bradley, 2016). Table 7 summarizes key TRNSYS components used in the system model.

**Table 7: Summary of key TRNSYS components**

| Component | TRNSYS Type | Notes |
|---|---|---|
| Building | Type 56 | Single family home in Montreal, Canada |
| Heat Pump | Type 927 | 4 ton, $COP_{Rated}$=4.28[1] |
| Ice Generator | Equation Type | Derived from Guilpart & Fournaison (2005) |
| Ice Tank | Type 217 (Custom Model) | Custom model, non-agitated ice slurry, Tamasauskas et al. (2012) |
| Warm Tank | Type 534 | Stratified storage, 4 nodes |
| PVT Array (Glazed) | Type 50 | Liquid PVT, $A_{Panel}$=1.43 $m^2$/panel |
| PVT Array (Unglazed) | Type 50 | Liquid PVT, $A_{Panel}$=1.33 $m^2$/panel |
| Heating Control | Type 23 | Separate PID control for each RF Loop |
| Radiant Flooring | Type 56 Active Layer | Separate Loops for all three levels |

[1] Rated at 0°C evaporator water temperature, 28°C condenser water temperature

*Building Model*. The system was integrated into a single family home in Montreal, QC, Canada. The geometry for the home was based on the Canadian Centre for Housing Technology (CCHT) test home (Swinton et al., 2005), and consists of two above ground floors and a finished basement with a heated floor area of 284 $m^2$. This home is considered representative of typical single family homes in Canada. The envelope of the home was then modified to meet an EnerGuide rating of ERS-86 (OEE, 2005). Details on the housing model and its development can be found in Kegel et al. (2012). Key envelope performance is summarized in Table 8.

**Table 8: House envelope properties**

| Envelope Property | Value |
|---|---|
| Roof RSI | 8.93 $m^2 \cdot °C/W$ |
| Wall RSI | 5.65 $m^2 \cdot °C/W$ |
| Basement Wall RSI | 4.95 $m^2 \cdot °C/W$ |
| Basement Slab RSI | 2.58 $m^2 \cdot °C/W$ |
| Window U-Value | 1.01 $W/m^2 \cdot °C$ |
| Infiltration | 0.75 $ACH_{50}$ |

To assess solar system performance it was also important to define two base case mechanical systems representing conventional and more efficient heating technologies. Table 9 summarizes key details for each system. In all cases, DHW draws are set to 233 L/day. Tank volumes for Base Case 2 are larger as this tank serves both DHW and radiant flooring loops. Heat pump performance was based on manufacturer data (Daikin, 2018).

**Table 9. Base case mechanical systems**

| | Base Case #1 | Base Case #2 |
|---|---|---|
| Heating System | Electric Baseboard | Air-Water Heat Pump (COP 3.29[†]), Radiant Flooring |
| Ventilation | HRV, 0.84 effectiveness | HRV, 0.84 effectiveness |
| DHW | Electric Conventional Tank | Air-Water Heat Pump + Tankless Electric (if needed) |
| | Tank Volume 0.23 $m^3$ | Tank Volume 0.50 $m^3$ (Serves RF and DHW loops) |

[†] Rated at 7°C outdoor dry bulb, 40°C inlet water temperature

Each base case is also equipped with a PV system sized for the full south-facing roof of the home (~41 $m^2$).

*PVT System*. PVT properties and parameters are provided in Table 10. It is assumed that all PV/PVT systems are grid tied, and can feed into the electricity grid when generation exceeds building demand. Provided information is derived from Solimpeks (2014), Notton et al. (2005), and Boubekri et al. (2009).

**Table 10: Parameters for PVT system**

| Parameter | Type/Value |
|---|---|
| PV Type | Mono-Crystalline |
| PV Efficiency | 14.88% |
| PV Efficiency Modifier | -0.0044 |
| Slope/Orientation | 40°/Due South |
| Panel Area | 1.43 $m^2$ (Glazed PVT & PV)<br>1.33 $m^2$ (Unglazed PVT) |

## 5. Results

Optimizations have been completed for several cases using an Intel Core i7-3840QM CPU @ 2.80 GHz. Results are presented first for an optimization of the PVT-only system, followed by an exploration of the optimal balance between PV and PVT collectors.

### *5.1 Overall Optimization Results: PVT Only Case*

Figure 3 compares the Pareto fronts for glazed and unglazed collectors. In nearly all cases, the glazed collector offers both superior lifecycle energy and cost performance, dominating candidate solutions using unglazed PVT. This result can primarily be attributed to the superior thermal performance of the glazed collector in Montreal, and the relatively small price and embodied energy increments between the two collector types. The only exception to this is at the far right of the graph, at the extreme minimum of lifecycle energy. In this situation, the primary thermal demands of the system are well matched using both the glazed and unglazed collector. As such, the extra electricity offered by the unglazed collector offers a slight improvement in lifecycle energy performance. While not included in this study, it is important to keep in mind that many regions include a feed-in tariff for onsite renewable generation. This would increase the attractiveness of PVT systems, especially for unglazed collectors, which prioritize electricity generation.

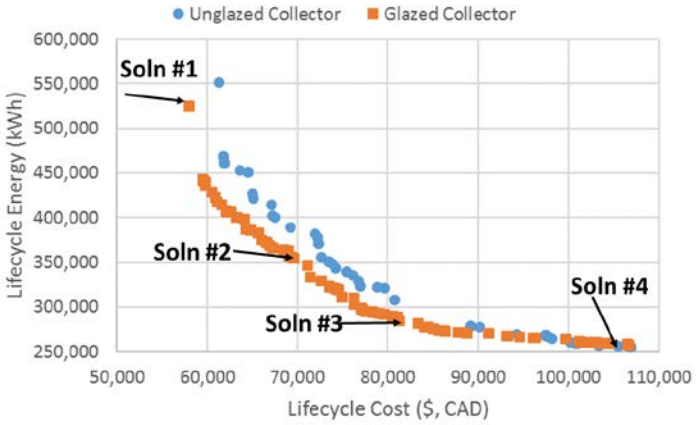


**Figure 3: Pareto fronts for glazed and unglazed PVT cases**

Table 11 summarizes optimized decision variables and objective functions for the four candidate solutions in Figure 3. Solutions with greater energy savings are associated with higher lifecycle costs. However, the relationship between increased costs and greater energy savings differs greatly over the Pareto front. Starting with a relatively small PVT array and storage capacity (Solution #1), it is possible to achieve a 32% reduction in lifecycle energy with only a 19% increase in lifecycle costs (Solution #2). The impact of additional investments becomes attenuated beyond this point, as moving from Solution #2 to Solution #3 yields a 19% reduction in lifecycle energy for a 17% increase in lifecycle costs. Finally, along the extreme right of the Pareto front, additional investments in equipment have little effect on lifecycle energy savings, with a 33% increase in lifecycle costs resulting in only a 12% reduction in lifecycle energy (Solution #3 to Solution #4). Increased collector area and tank storage volumes appears to be the main drivers towards reduced lifecycle energy (and increased lifecycle costs).

**Table 11: Candidate solutions from the combined Pareto front**

| | Solution | | | |
|---|---|---|---|---|
| | **1** | **2** | **3** | **4** |
| **PVT Type** | Glazed | Glazed | Glazed | Unglazed |
| **$N_{collectors}$** | 6 | 24 | 29 | 31 |
| **$V_{Ice}$ ($m^3$)** | 0.50 | 0.60 | 1.20 | 4.30 |
| **$V_{WWST}$ ($m^3$)** | 0.33 | 0.33 | 0.97 | 1.66 |
| **$m_{col}$ ($kg/s \cdot m^2$)** | 0.0071 | 0.0071 | 0.0156 | 0.0321 |
| **LCC ($, CAD)** | 58,000 | 69,000 | 80,500 | 106,900 |
| **LCE( kWh)** | 524,800 | 356,900 | 289,800 | 255,400 |

Table 12 presents the distribution of lifecycle energy by system element. It is immediately evident that the distribution of energy by component, and between the equipment and operations phases, changes significantly between the four solutions presented. As solutions move towards lower lifecycle energy, a greater portion of this total is associated with the embodied energy of the system components, especially the PVT collectors. Also evident is the lower embodied energy of the storage tanks, which never exceed 9% of total system lifecycle energy. Embodied energy for the pumps remains constant, as there is little variation in the mass between the pump sizes used in this case study.

**Table 12: Division of lifecycle energy by component for candidate solutions**

| | Lifecycle Energy (kWh) | | | | | | | |
|---|---|---|---|---|---|---|---|---|
| | **1** | | **2** | | **3** | | **4** | |
| **Total System** | 524,800 | | 356,900 | | 289,800 | | 255,400 | |
| **PVT** | 35,810 | 7% | 141,210 | 40% | 170,490 | 59% | 164,560 | 64% |
| **Ice Tank** | 3,800 | 1% | 4,140 | 1% | 6,410 | 2% | 14,120 | 6% |
| **Warm Tank** | 3,010 | 1% | 3,010 | 1% | 5,760 | 2% | 7,960 | 3% |
| **Pumps** | 110 | <1% | 110 | <1% | 110 | <1% | 110 | <1% |
| **Operations** | 482,070 | 92% | 208,430 | 58% | 107,030 | 37% | 68,650 | 27% |

Table 13 presents similar information for lifecycle cost. From the economic perspective, there is also a shift from (i) low initial investment and high operating costs, to (ii) a far greater initial expenditure on the system, but with lower costs during operations. In contrast to lifecycle energy results, a far more significant proportion of costs is also associated with larger storage tanks, especially for Solutions #3 and #4. This breakdown of lifecycle costs can be particularly useful for designers and building owners: A long-term owner/operator may prefer to have a higher initial expenditure while saving on operating costs and hedging against future utility price fluctuations, especially when subsidies for efficient equipment are available.

**Table 13: Division of lifecycle cost by component for candidate solutions**

| | Lifecycle Cost ($, CAD) | | | | | | | |
|---|---|---|---|---|---|---|---|---|
| | **1** | | **2** | | **3** | | **4** | |
| **Total System** | $58,000 | | $69,000 | | $80,500 | | $106,900 | |
| **PVT** | $10,510 | 18% | $42,050 | 61% | $50,820 | 63% | $51,600 | 48% |
| **Ice Tank** | $5,880 | 10% | $6,400 | 9% | $10,620 | 13% | $32,920 | 31% |
| **Warm Tank** | $4,770 | 8% | $4,770 | 7% | $9,290 | 12% | $14,170 | 13% |
| **Pumps** | $1,130 | 2% | $1,280 | 2% | $2,490 | 3% | $3,220 | 3% |
| **Operations** | $35,710 | 62% | $14,500 | 21% | $7,280 | 9% | $4,990 | 5% |

Table 14 compares the annual energy performance by end use for each candidate solution, and the two base cases defined in Table 9. While all candidate solutions offer reductions over the first base case (electric resistance elements for heating and DHW), it is interesting to note that only Solutions #3 and #4 provide net annual energy use reductions versus the air-water heat pump case (Base #2). Each of these two solutions takes a different approach to achieving lower lifecycle energy. In Solution #3, the glazed PVT area is maximized in order to increase thermal energy supply and reduce energy use for heating and DHW. Solution #4 uses unglazed collectors with a larger ice tank volume, sacrificing performance in heating and DHW modes in order to increase electricity production. It is also important to note the impact of cooling the PV panels: In Solution #4, annual PV production is boosted by approximately 60 kWh, although this increase is mitigated somewhat by limited solar loop operations during the warmer months when there is reduced demand for heating and DHW in the building.

**Table 14: Annual energy use for candidate solutions**

| | Base #1 | Base #2 | Soln #1 | Soln #2 | Soln#3 | Soln #4 |
|---|---|---|---|---|---|---|
| **Heating+DHW (kWh)** | 13,780 | 6,970 | 8,260 | 5,750 | 4,410 | 4,580 |
| **Fans+Pumps (kWh)** | N/A | 990 | 930 | 960 | 980 | 1,000 |
| **Lighting+Receptacles (kWh)** | 4,480 | 4,480 | 4,480 | 4,480 | 4,480 | 4,480 |
| **Total Electricity Use (kWh)** | 18,260 | 12,440 | 13,670 | 11,190 | 9,870 | 10,060 |
| **Total PV Generation (kWh)** | 8,280 | 8,280 | 1,610 | 5,970 | 7,190 | 8,340 |
| **Net Electricity Use (kWh)** | 9,980 | 4,160 | 12,060 | 5,220 | 2,680 | 1,720 |

## 5.2 Overall Optimization Results: PVT & PV Case

In addition to the PVT-only optimization, a second optimization was performed to determine the best balance between PV and glazed PVT collectors. This optimization was run using the same objective functions and optimization parameters as the previous case. However, instead of leaving unused roof space if the PVT array area was less than its maximum, the remaining available roof space was instead covered with PV panels. Each PV panel was assumed to have an identical area to the glazed PVT panel (1.43 $m^2$), with the total number of PV panels then:

$$N_{PV} = 29 - N_{PVT} \quad \text{(eq. 4)}$$

Where $N_{PV}$ is the number of PV panels, and 29 represents the maximum number of solar collectors (PV or PVT) that can be integrated onto the south facing roof. The embodied energy and cost of the PV panels were then included in the optimization to appropriately assess the impact of their integration.

Figure 4 shows the Pareto front for this new optimization case. It is immediately evident this front is far shallower than for the glazed PVT-only case. The addition of PV, via its electrical generation capacity, greatly reduces the lifecycle energy use of the lowest-cost solutions. For solutions at the low end of lifecycle costs, adding PV results in only a small net cost increase in comparison to the PVT-only case, primarily because utility bills are reduced. As lifecycle cost increases, solutions tend to closely approach the PVT-only case, as higher-cost candidates are associated with near-maximum PVT areas.

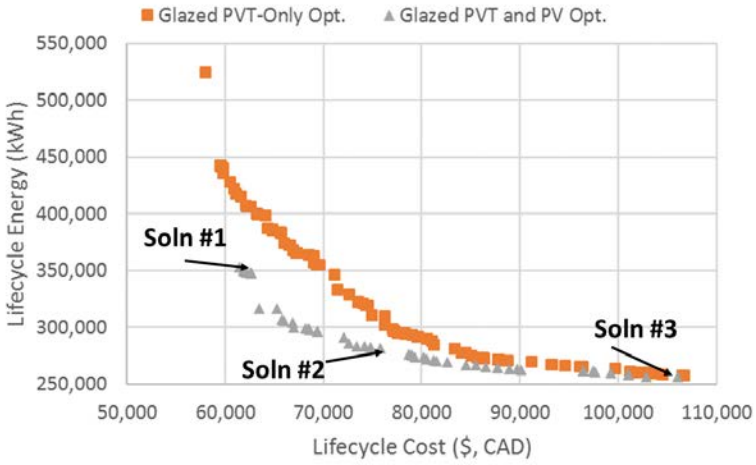


**Figure 4: Pareto front for PVT & PV case**

Table 15 summarizes the decision variables and objective function values for each of the three solutions identified in Figure 4. As with the PVT-only case, solutions are driven towards lower lifecycle energy by the addition of PVT collectors and increased storage tank volumes. However, the integration of glazed PVT appears to have both a lower and an upper limit. If less than 7 PVT collectors are used, increased system energy use for heating and DHW outweighs the additional electricity that could be obtained from a greater number of PV panels. At the upper limit, the system is able to achieve suitable thermal supply with 24 PVT collectors, when combined with sufficiently large storage tanks. Integrating additional PVT panels beyond this point results in a net increase in lifecycle energy, primarily because the reductions in electricity generation outweigh additional savings for heating and DHW.

**Table 15: Candidate solutions for PVT & PV optimization**

| | Solution | | |
|---|---|---|---|
| | **1** | **2** | **3** |
| **$N_{collectors}$** | 7 | 18 | 24 |
| **$V_{Ice}$ ($m^3$)** | 0.40 | 1.10 | 4.60 |
| **$V_{WWST}$ ($m^3$)** | 0.41 | 1.53 | 2.12 |
| **$m_{col}$ ($kg/s \cdot m^2$)** | 0.0153 | 0.0108 | 0.0143 |
| **LCC ($, CAD)** | 62,000 | 75,800 | 106,100 |
| **LCE( kWh)** | 349,500 | 281,500 | 256,200 |

Table 16 compares the annual energy performance of each system, along with the corresponding electricity generation and net electricity use. Similar to the PVT-only case, all systems offer net energy use reductions in comparison to the electrical resistance base case (Base #1), while only the final two solutions present savings vs. the more efficient heat pump system (Base #2). However, these reductions are now more drastic given that the complete roof has some form of PVT or PV, with net energy use savings ranging from 31% with Solution #2 to 58% with Solution #3. It is also interesting to note the strong energy performance in heating/DHW for Solution #3. Although the number of PVT collectors is less than a similar solution in the PVT-only case (Solution #3, PVT-only), increased storage tank volumes are able to achieve an additional 15% energy use reduction for heating and DHW (46% vs. the air-water base case (Base #2)).

**Table 16: Annual energy performance of candidate solutions for PVT&PV optimization**

| | **Base #1** | **Base #2** | **Soln #1** | **Soln #2** | **Soln #3** |
|---|---|---|---|---|---|
| **Heating+DHW (kWh)** | 13,780 | 6,970 | 7,900 | 5,140 | 3,770 |
| **Fans+Pumps (kWh)** | N/A | 990 | 940 | 970 | 980 |
| **Lighting+Receptacles (kWh)** | 4,480 | 4,480 | 4,480 | 4,480 | 4,480 |
| **Total Electricity Use (kWh)** | 18,260 | 12,440 | 13,320 | 10,590 | 9,230 |
| **Total PV Generation (kWh)** | 8,280 | 8,280 | 8,150 | 7,700 | 7,500 |
| **Net Electricity Use (kWh)** | 9,980 | 4,160 | 5,170 | 2,890 | 1,730 |

Table 17 compares the lifecycle performance of the three solutions with the air-water heat pump base case. Both Solutions #2 and #3 are able to offer important lifecycle energy savings, driven by improved performance in heating and DHW modes. These reductions however, are less dramatic than those for annual energy use, primarily because of the higher embodied energy associated with the PVT panels and storage tanks.

It is also interesting to note the substantially lower lifecycle cost offered by the air-water heat pump (assuming that heat pumps would cost an identical amount for all cases), with this system dominating a number of solutions along the Pareto front. This result also highlights the importance of a properly sized system: Solar-assisted heat pumps with insufficient thermal supply or storage will likely result in increased lifecycle energy use and cost vs. a conventional HP + PV, as shown when comparing the base case with Solution #1.

**Table 17: Comparison life lifecycle performance for base case and candidate solutions**

| | **Base #2** | **Soln #1** | **Soln #2** | **Soln #3** |
|---|---|---|---|---|
| **LCC ($, CAD)** | $46,900 | $62,000 | $75,800 | $106,100 |
| **LCE(kWh)** | 293,800 | 349,500 | 281,500 | 256,200 |

## 6. Conclusions

This paper presents the multi-objective optimization of a novel solar heat pump system according to the competing objectives of lifecycle energy and cost. The optimization methodology was first applied to determine optimal system sizing, assuming that the system only used PVT panels. Results showed a clear trade-off between increased investment for PVT panels and storage tank volumes, and reduced lifecycle energy use of the system. However, this relationship was shown to follow a trend of diminishing returns, with limited additional energy savings beyond certain collector areas and tank volumes. In general, glazed PVT collectors were found to dominate the Pareto front, except for solutions at the extreme minimum of lifecycle energy use, where unglazed collectors were preferred due to their lower cost and increased electricity-generating potential.

A second optimization explored the balance between PV and glazed PVT collectors. Solutions in the Pareto front were found to weigh (i) thermal energy supply from the PVT panels with (ii) increased electricity generating potential from the PV panels. System comparisons demonstrated the potential of the proposed solar heat pump, when sized appropriately, to offer substantial lifecycle energy savings in comparison to a base case using an air-water heat pump with PV. However, the base case heat pump and PV combination was found to offer attractive lifecycle economics, while still providing superior energy performance vs. solar heat pump systems with more limited thermal supply and storage capacity.

These results represent an initial examination of system performance for a single building type (single family home) and city (Montreal, QC). It is likely that system deployment in larger buildings will offer greater potential energy use and cost reductions, due to the ability to more easily integrate significant collector areas and storage volumes, and reduce capital investment via economies of scale. Regions with higher electricity rates will also result in the PVT systems offering a more economically viable alternative to conventional heat pumps, as the monetary impacts of energy savings will hold greater significance.

## 7. References

Bornatico, R., Pfeiffer, M., Andreas W., Guzzella L., 2012. Optimal sizing of a solar thermal building installation using particle swarm optimization. Energy 41, 221-228. https://doi.org/10.1016/j.energy.2011.05.026

Boubekri, M., Chaker, A., Cheknane A., 2009. Numerical approach for performance study of hybrid PV/Thermal collector. Revue des Energies Renouvelables 12, 355-368. Available at: https://www.cder.dz/spip.php?article370

Bradley, D., 2016. How to set simulation start and timestep to avoid error. Available at: http://onebuilding.org/ [Accessed Jun. 2016]

Carbonell, D., Phillippen, D., Haller, M.Y., Brunold, S., 2016. Modeling of an ice storage buried in the ground for solar heating applications: Validations with one year of monitored data from a pilot plant. Solar Energy 125, 398-414. https://doi.org/10.1016/j.solener.2015.12.009

Chow, T., Ji, J., 2012. Environmental Life-Cycle Analysis of Hybrid Solar Photovoltaic/Thermal Systems for Use in Hong Kong. International Journal of Photoenergy 2012, 101968. http://dx.doi.org/10.1155/2012/101968

ClimateMaster, 2010. TMW Water-To-Water Series. Available at: http://www.climatemaster.com [Accessed Jan. 2012]

Daikin, 2018. ERLQ-CV3. Available at: https://www.daikin.co.uk/en_gb/products/ERLQ-CV3.html [Accessed Spt. 2018]

Deb K., Pratap A., Agarwal S., Mayarivan T., 2002. A Fast and Elitist Multiobjective Genetic Algorithm: NSGA-II. IEEE Transactions on Evolutionary Computation 6, 182-197. https://doi.org/10.1109/4235.996017

Dott, R., Afjei, T., 2014. Evaluation of Solar & Heat Pump System Combinations. In Proceedings of IEA HPC 2014, IEA HP.

EnergyHub.org, 2018. Average Cost of Solar Panels in Canada 2018. Available at: https://solarpanelpower.ca/cost-solar-panels-canada/ [Accessed August 2018]

Guilpart, J., Fournaison, L., 2005. The Control of Ice Slurry Systems. In Kauffeld, M., Kawaji, M., Egolf, P. (Eds.), Handbook on Ice Slurries. International Institute of Refrigeration, Paris, pp. 281-285.

Haus & Solar, 2017. Volther PowerTherm PV-T Hybrid Collector. Available at: http://www.hausundsolar.de/Volther-PowerTherm-PV-T-Hybrid-Collector-185W [Accessed February 2017]

Hydro Quebec, 2017. Rates for residential customers (domestic rates). Available at: http://www.hydroquebec.com/residential/ [Accessed January 2017]

IEA Heat Pump Centre (IEA HPC), 2012. The role of heat pumps in net zero energy buildings. IEA Heat Pump Centre Newsletter 30, 3. Available at: https://heatpumpingtechnologies.org/publications/52485/

Kegel, M., Sunye, R., Tamasauskas, J., 2012. Lifecycle Cost Comparison and Optimisation of Different Heat Pump Systems in the Canadian Climate. In Proceedings of eSim 2012 Halifax, IBPSA Canada, 492-505.

Klein S. A., et al., 2010. TRNSYS 17 – A TRaNsient SYstem Simulation program user manual. University of Wisconsin-Madison Solar Energy Laboratory, Madison, WI, USA.

Leckner, M., 2008. Life cycle energy and cost analysis of a net zero energy house using solar combisystem. Master Thesis, Concordia University, Montreal, Canada.

MathWorks, 2018. MATLAB - The Language of Technical Computing Available at: http://www.mathworks.com/products/matlab/ [Accessed Sept. 2018]

Ng Cheng Hin, J., 2013. Life Cycle Optimization of a Residential Solar Combisystem for Minimum Cost, Energy Use, and Exergy Destroyed. Master Thesis, Concordia University, Montreal, Canada.

Ng Cheng Hin J., Zmeureanu R., 2014. Optimization of a residential solar combisystem for minimum life cycle cost, energy use, and exergy destroyed. Solar Energy 100, 102-113. https://doi.org/10.1016/j.solener.2013.12.001

Notton, G., Cristofari, C., Mattei, M., Poggi, P., 2005. Modelling of a double-glass photovoltaic module using finite differences. Applied Thermal Engineering 25, 2854-2877. https://doi.org/10.1016/j.applthermaleng.2005.02.008

Office of Energy Efficiency (OEE), 2005. EnerGuide for New Houses: Administrative and Technical Procedures. Natural Resources Canada, Ottawa, Canada. Available at: http://www3.cec.org/islandora-gb/en/islandora/object/greenbuilding%3A43

Palonen, M., Hamdy, M., Hasan, A., 2013. MOBO A new software for multi-objective building performance optimization. Proceedings of BS 2013, IBPSA, Chambery, France. Available at: http://www.ibpsa.org/proceedings/bs2013/p_1489.pdf

Renewable Energy Hub, 2018. PowerVolt. Available at: https://www.renewableenergyhub.co.uk/product/powervolt.html [Accessed August 2018]

Rey A., Zmeureanu R., 2016. Multi-objective optimization of a residential solar thermal combisystem. Solar Energy 139, 622-632. https://doi.org/10.1016/j.solener.2016.10.008

RS Means, 2013. RS Means Mechanical Cost Data 2013. Reed Construction Data, Norwell, USA.

Solimpeks, 2014. Installation, Operation, and Maintenance: Solar Panels. Available at: http://www.solimpeks.com, [Accessed Mar. 2016]

Spence, W., Kultermann, E., 2017. Construction Materials, Methods, and Techniques, fourth ed. Cengage Learning, Boston.

Swinton, M.C., Entchev, E., Szadkowski, F., Marchand, R., 2003. Benchmarking twin houses and assessment of the energy performance of two gas combo heating systems. Canadian Centre for Housing Tech, Ottawa, Canada. Available at: http://www.ccht-cctr.gc.ca/eng/projects/gas_combo.html

Tamasauskas, J., Poirier, M., Zmeureanu, R., Sunye, R., 2012. Modeling and optimization of a solar assisted heat pump using ice slurry as a latent storage material. Solar Energy 86, 3316-3325. https://doi.org/10.1016/j.solener.2012.08.021

Tamasauskas, J., Poirier, M., Zmeureanu, R., Kegel, M., Sunye, R., McDonald, E., 2016. The Potential of Liquid-based BIPVT and Ice Storage for High Performance Housing in Canada. In Proceedings of 4th International High Performance Buildings Conference, Purdue University, West Lafayette, IN, USA. Available at: https://docs.lib.purdue.edu/ihpbc/208/

Trinkl, C., Zorner, W., Hanby, V., 2009. Simulation study on a Domestic Solar/Heat Pump Heating System Incorporating Latent and Stratified Thermal Storage. J. Sol. Energ.-T. ASME 131, 041008-1 to 041008-8. http://dx.doi.org/10.1115/1.3197845